Broadband Direct UVA Irradiance Measurement for Clear Skies Evaluated Using a Smartphone

D. Igoe[1*] & A.V. Parisi[1]

[1]Faculty of Health, Engineering and Sciences, University of Southern Queensland, Toowoomba. Australia

*Corresponding author: damienpaul@gmail.com

Short Title: Broadband Direct UVA Irradiances

Abstract

UVA wavelengths (320-400 nm) have been implicated in recent studies to contribute to melanoma induction and skin photoaging in humans and damage to plants. The use of smartphones in UVA observations are a way to supplement measurements made by traditional radiometric and spectroradiometric technology. Although the smartphone image sensor is not capable of determining broadband UVA irradiances, these can be reconstructed from narrowband irradiances, which the smartphone, with narrowband and neutral density filters, can quantify with discrepancies not exceeding 5%. Three models that reconstruct direct broadband clear sky UVA were developed from narrowband irradiances derived from smartphone image sensor pixel data with coefficients of determination of between 0.97 and 0.99. Reasonable accuracy and precision in determining the direct broadband UVA was maintained for observations made with solar zenith angles as high as 70°. The developed method has the potential to increase the uptake of the measurement of broadband UVA irradiances.

Introduction

The UVA wavelengths (320-400 nm) are implicated as damaging to human health as possibly contributing to melanoma induction[(1)]. Additionally, the UVA waveband contributes to premature skin aging[(2)]. The UVA has also been reported to influence the effects of the UV radiation on damage to plants[(3)]. The UVA waveband is also transmitted to varying amounts through glass and plays a role in UV irradiances to humans resulting from UV transmitted through glass[(4)]. The percentage of transmitted UVA is influenced by the thickness, type of glass and whether or not the glass is laminated or tinted[(5-8)]. Critically, the ozone absorption coefficients are significantly less in the UVA compared to the UVB and at 334 nm are 0.8% of that at 297 nm[(9)].

The techniques of radiometry and spectroradiometry are employed in the measurement of UVA irradiances[(10)]. These include the measurement of the diffuse, direct and global (direct + diffuse) irradiances. The irradiances at the three wavelengths of 320, 340 and 380 nm have been employed in clear sky conditions for the evaluation of solar irradiances[(11)]. Another approach to evaluate the UVA irradiances has been the development of a model that employs the measured irradiance at 368 nm and the empirically determined irradiances in the UVA waveband and at 368 nm[(12)]. Other approaches have employed the use of cloud modification factors to the clear sky irradiances for the evaluation of the UVA[(13,14)].

The image sensors on smartphones have been reported as having a response in the UVA waveband[(15)]. This quantifiable response has led to the development of a method for evaluation of aerosol optical depth at UVA wavelengths[(16,17)]. The widespread uptake and use of smartphones has the potential to increase the uptake of the measurement of broadband UVA irradiances. However, in order to achieve this it is necessary to overcome the problem of a smartphone image sensor not being directly capable of measuring broadband UVA due to some phone sensors not possessing a flat response in the UVA. Another limitation is that all phone image sensors respond differently to UV wavelengths. This paper extends the previous research by developing a method for the evaluation of the direct sun, clear sky broadband UVA irradiances with a smartphone.

Materials and Methods

The approach employed in this research was to develop a model to evaluate the broadband direct sun UVA irradiances from the direct sun narrowband irradiances measured with a smartphone at 320, 340 and 380 nm. Further data on the direct sun broadband UVA were then collected to validate the model developed against a calibrated ultraviolet meter (model 3D, Solar Light, USA). This meter was calibrated for the UVA against a calibrated Bentham spectroradiometer (model DTM300, Bentham Instruments Inc, UK). The input data for the model were the direct sun narrowband UVA irradiances at 320, 340 and 380 nm. These were measured with a LG L3 smartphone (LG Electronics, Seoul, South Korea) image sensor with the image intensity for each measurement calibrated with a Microtops sunphotometer (Model E540, Solar Light, USA) for the narrow band irradiances at the respective wavelengths. This instrument measures the direct sun irradiances at each of the wavelengths with a FWHM of 2 nm.

Data for Evaluation of Direct UVA Irradiances

Igoe et al.[16,17] have demonstrated that there exists a very strong correlation between the natural log of narrow bandwidth irradiances measured by the Microtops and the natural log of the product of the image sensor average grayscale over the same narrow bandwidth, the Earth-sun distance factor and the fourth power of the cosine of the sun zenith angle.

The three target narrowband wavelengths employed for this research to evaluate the broadband UVA irradiances were 320 nm, 340 nm and 380 nm. These were selected as they correspond to the narrowband irradiances measured on the Microtops. To ensure that direct solar measurements were made on the smartphone and ultraviolet meter, 7 cm length black tubes of 2.5 cm diameter were used over the respective optics. Narrowband interference filters (Melles Griot, supplier Lastek, Australia) with centre wavelengths of 320, 340 and 380 nm respectively and a FWHM of 10 nm were employed on the smartphone to provide the respective wavelengths. These were coupled in a light tight arrangement including the 7 cm black tube with a 1% neutral density filter (Asahi Filters, Tokyo, Japan) to prevent the saturation of the image sensor(16,17). Additionally, an ND2 neutral density filter (Bentham Instruments, Inc. UK) was used for 380 nm observations due to the higher irradiance at this waveband(16,17).

Direct sun measurements were performed at 20 minute intervals, between 9:00 am and noon on cloud free days, from late May to late June on a high school oval in Gladstone, Queensland (23.91°S 151.27°E) with a solar zenith angle range of 67° to 47°. Two sets of observations were made, three weeks apart to obtain the data to develop the model for the evaluation of the direct UVA irradiances. The atmospheric ozone range was 262 to 294 DU. The aerosol optical depth ranged from 0.16 to 0.21 and 0.06 to 0.09 at 340 and 380 nm respectively.

The smartphone and ultraviolet meter sensors were oriented in the same direction as that of the Microtops, using the sun alignment optics on the sun photometer to ensure all three instruments recorded direct sun irradiances for each measurement. The data recorded include the image data from the smartphone image sensor with 3 images of the direct sun at each of 320, 340 and 380 nm taken at each measurement time, the irradiances recorded at 320 nm, 340 nm and 380 nm; aerosol optical depth at 340 nm and 380 nm and solar zenith angle from the Microtops and the total direct UVA irradiances from the ultraviolet meter. Each set of measurements were taken within 5 minutes, with minimal change in the UVA irradiances over that time of the order of less than 4% at 9 am and less than 1% at noon.

A previously described smartphone app that was written to determine the mean and standard deviation of the grayscale (intensity) response detected by the image sensor above a dark noise threshold(17) was employed, where the grayscale was calculated using:

$$Grayscale = 0.299(red) + 0.587(green) + 0.114(blue) \tag{1}$$

The terms red, green and blue are the average of the pixel values in the respective channels(18). Recent studies by Igoe et al.(19), demonstrated that the magnitude of thermally-induced dark noise does not vary significantly through daytime temperatures; hence can be considered as a constant threshold. Average grayscale responses were taken above the dark noise threshold, over the solar disk.

Model Development and Evaluation

The ultraviolet meter total direct UVA was compared to the sum of smartphone-derived irradiances ($I_{320} + I_{340} + I_{380}$) where each of the terms is the irradiances at each of 320, 340 and 380 nm respectively. Additionally, the broadband UVA was compared to the irradiances for each wavelength individually, in a similar manner to Grant and Slusser(12) to determine if any wavelength (or their sum) would provide an accurate model for broadband direct sun UVA. Another model tested was to use the trapezoidal method in determining the relative irradiance proportions each narrowband wavelength contributes to the broadband direct sun UVA. The sum therefore becomes $10I_{320} + 30I_{340} + 40I_{380}$, this model is denoted as I_{trap}.

Once calibrations and development of the model were complete over two trial days, verification tests were performed to validate the accuracy and precision of the broadband direct sun UVA model developed in conditions where the AOD were different. This data were collected on relatively cloud free days on the 29th June and 7th July 2014 between 8 am and noon with a solar zenith angle range of 70° to 44°. The atmospheric ozone range was 267 to 291 DU and the average aerosol optical depth range was 0.15 and 0.05 for 340 nm and 380 nm respectively.

Results and Discussion

The smartphone image sensor was first calibrated to each of the natural log of the direct sun irradiances recorded by the Microtops at 320 nm, 340 nm and 380 nm. The calibration followed the general approach established by Igoe et al.[16] experimentally and used in an app to detect aerosol optical depth[17]. The general relationship between the natural log of direct irradiance from the Microtops ($I_{Microtops}$) to the 'cosine grey' value derived from the average of the grayscale values (Y_{av}) above a threshold from the smartphone is presented below. This value represents the average over approximately 1600 pixels in each image and averaged over three images.

$$\ln I_{Microtops} = m \ln(Y_{av} D^2 \cos^4 SZA) + c \qquad (2)$$

where D^2 represents the Sun-Earth distance correction factor[20], SZA is the solar zenith angle and *m* and *c* are the correlation gradient and intercept respectively.

The correlations between the Microtops and smartphone derived values were very strong for all three target wavelengths, with coefficients of determination of 0.99, 0.99 and 0.97 for 380 nm, 340 nm and 320 nm observations respectively where the x axis values of smartphone cosine grey are $\ln(Y_{av} D^2 \cos^4 SZA)$.

A source of variation for the UVA irradiances is the aerosol optical depth. The calibration observations were made on days with different aerosol optical depths, as measured by the Microtops. These were 0.189±0.013 and 0.075±0.006 for 340 nm and 380 nm respectively. Another source of variation is the differences in the image sensors between different phones and different models. In a similar manner to how individual UV radiometers need calibration, individual phone image sensors will require calibration.

The smartphone derived direct sun UVA irradiances for each of the models were compared to the direct sun UVA irradiances measured with the meter. The coefficient of determination of broadband direct sun UVA comparisons varied considerably with wavelength (Table 1). For practicality, each regression was set to have an intercept of zero to better describe the relationship between broadband direct sun UVA and smartphone derived narrowband irradiances.

>Table 1<

The very strong correlation observed for the model bases I_{380}, (I_{320} + I_{340} + I_{380}) and I_{trap} suggest that any of these could be used as a proxy to model the total direct clear sky UVA irradiances using smartphone image sensor derived irradiances, the derived regressions for the LG L3 smartphone are in equations 3, 4 and 5 and the regression lines are in Figures 1, 2 and 3 respectively.

$$UVA_{direct} = 12.01 I_{380} \tag{3}$$

$$UVA_{direct} = 8.95(I_{320} + I_{340} + I_{380}) \tag{4}$$

$$UVA_{direct} = 0.25 I_{trap} \tag{5}$$

>Figure 1<

>Figure 2<

>Figure 3<

The results for evaluation of broadband UVA were validated on clear sky days where the AOD was less than that observed in the calibration phase, recording averages of 0.152±0.013 and 0.049±0.002 for 340 nm and 380 nm respectively. When the validation data was modelled with the calibration data and compared to the direct sun UVA detected by the ultraviolet meter, there were no measurable effects of the lower AOD. Additionally, six measurements were taken at SZAs of over 60°, including as high as 70° (air mass 2.92) and exhibited no significant discrepancies, as shown in Figures 4 to 6.

>Figure 4<

>Figure 5<

>Figure 6<

Discrepancies between the direct sun UVA models and values recorded by the ultraviolet meter typically were within approximately 4%, increasing as the solar zenith angle increased beyond 60°. The three models demonstrated similar precision in determining direct UVA irradiances (Figure 7). The model based on I_{380} is easier to implement in terms of the input data required. This model should be applicable for the clear sky cases where there are not significant variations in the relative shape of the UVA spectrum. The other two models that include I_{320} and I_{340} take into account variations in the relative shape of the UVA spectrum.

>Figure 7<

Conclusion

A method has been developed and validated to evaluate the direct sun clear sky irradiances from narrowband direct sun smart phone derived images. Three accurate and precise models were employed to reconstruct the direct sun broadband UVA clear sky irradiances from narrowband irradiance observations made using a smartphone image sensor. Narrowband irradiances were calibrated against standard instrumentation. Additional calibration was made using an ultraviolet meter to reconstruct the direct sun UVA clear sky irradiances. Calibration and validation observations demonstrated that the reconstruction provides reliable direct sun, clear sky UVA irradiances at solar zenith angles up to 67°. The developed method has the potential to increase the uptake of the measurement of broadband UVA irradiances. Examples of where they can be utilised are in schools for both the teaching of physics principles and for the education of children about solar radiation.

References

1. Noonan, F. P., Zaidi, M. R., Wolnicka-Glubisz, A., Anver, M. R., Bahn, J., Wielgus. A., Cadet, J., Douki, T., Mouret, S., Tucker, M. A., Popratiloff, A., Merlino, G., De Fabo, E. C., Melanoma induction by ultraviolet A but not ultraviolet B radiation requires melanin pigment. Nature Communications, 3:884 doi: 10.1038/ncomms1893 (2012).
2. McCullough, J. L. and Kelly, K. M. Prevention and treatment of skin ageing. Annals NY Acad. Sci. 1067, 323-331 (2006).
3. Flint, S. D. and Caldwell, M. M. A biological spectral weighting function for ozone depletion research with higher plants. Physiol. Plant, 117, 137-144 (2003).
4. Wong, C. F. and Parisi, A. V. Measurement of UVA exposure to solar radiation. Photochem. Photobiol. 63, 807-810 (1996).
5. Duarte, I., Rotter, A., Malvestiti, A. and Silva, M. The role of glass as a barrier against the transmission of ultraviolet radiation: an experimental study. Photodermatol. Photoimmunol. Photomed, 25, 181-184 (2009).
6. Almutawa, F. and Buabbas, H. Photoprotection clothing and glass. Dermatol. Clin.. 32, 439-448 (2014).
7. Parisi, A. V., Turnbull, D. J. and Kimlin, M. G. Dosimetric and spectroradiometric investigations of glass filtered solar UV. Photochem. Photobiol. 83, 777-781 (2007).
8. Hampton, P. J., Farr, P. M., Diffey, B. L. and Lloyd, J. J. Implication for photosensitive patients of ultraviolet A exposure in vehicles. Br. J. Dermatology, 151, 873-876 (2004).

9. Daumont, D., Brion, J., Charbonnier, J & Malicet, J. Ozone UV spectroscopy I: Absorption cross-sections at room temperature. J. Atmospheric Chemistry, 15, 145-155 (1992).
10. Diffey, B. L. Sources and measurement of ultraviolet radiation. Methods, 28, 4-13, (2002).
11. Anav, A., Rafanelli, C., Di Menno, I. and Di Menno, M. An algorithm to evaluate solar irradiance and effective dose rates using spectral UV irradiance at four selected wavelengths. Rad. Prot. Dosim. 111, 239-250 (2004).
12. Grant, R. and Slusser, J. Estimation of ultraviolet-A irradiance from measurement of 368 nm spectral irradiance. J. Atm. Ocean. Tech. 22, 1853-1863 (2005).
13. Jacovides, C. P., Tymvios, F. S., Assimakopoulos, V. D., Kaltsounides, N. A., Theoharatos, G. A. and Tsitouri, M. Solar global UVB (280-315 nm) and UVA (315-380 nm) radiant fluxes and their relationships with broadband global radiant flux at an eastern Mediterranean site. Agric. For. Meteorol. 149, 1188-1200 (2009).
14. Parisi, A. V., Downs, N. and Turner, J. Evaluation of the cloudy sky solar UVA radiation exposures. J. Photochem. Photobiol. B: Biol. 138, 141-145 (2014).
15. Igoe, D., Parisi, A. V. and Carter, B. Characterisation of the UVA response of a smart phone. Photochem. Photobiol. 89, 215-218 (2013).
16. Igoe, D., Parisi, A. V. and Carter, B. Evaluating UVA aerosol optical depth using a smartphone camera. Photochem. Photobiol. 89, 1244-1248 (2013).
17. Igoe, D., Parisi, A. V. and Carter, B. Smartphone-based Android app for determining UVA aerosol optical depth and solar irradiances. Photochem. Photobiol. 90, 233-237 (2014).
18. Malacara, D. Color Vision and Colorimetry: Theory and Applications. Bellingham, SPIE Press (2002).

19. Igoe, D., Parisi, A. V. and Carter, B. A method for determining the dark response for scientific imaging with smartphones. Instrumentation Science and Technology, 42, 586-592 (2014).

20. Morys, M., Mims III, F., Hagreup, S., Anderson, S., Baker, A., Kia, J. and Walkup, T. Design, calibration, and performance of MICROTOPS II handheld ozone monitor and sun photometer. J. Geophys. Res. 106, 14573-14582 (2001).

Tables

Table 1: Coefficient of determination of narrowband wavelength based models for broadband direct sun UVA irradiances.

Model base	R^2
I_{320}	0.127
I_{340}	0.819
I_{380}	0.987
$I_{320} + I_{340} + I_{380}$	0.968
I_{trap}	0.984

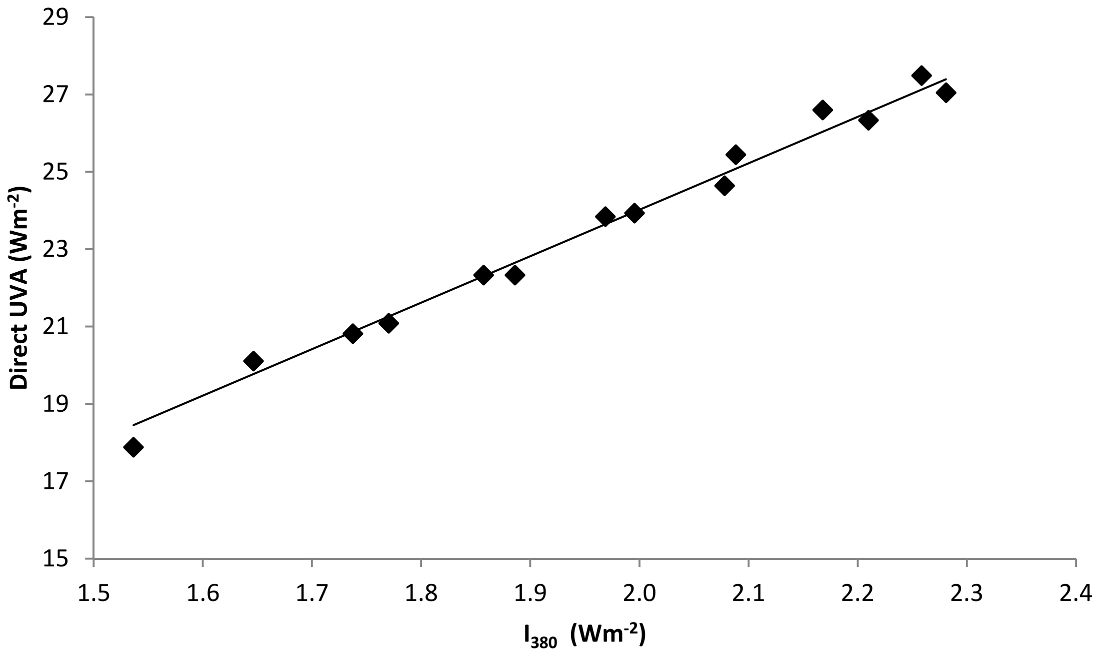

Figure 1: Model for the determination of the broadband direct sun UVA irradiances from the smartphone derived narrowband direct sun irradiances at 380 nm.

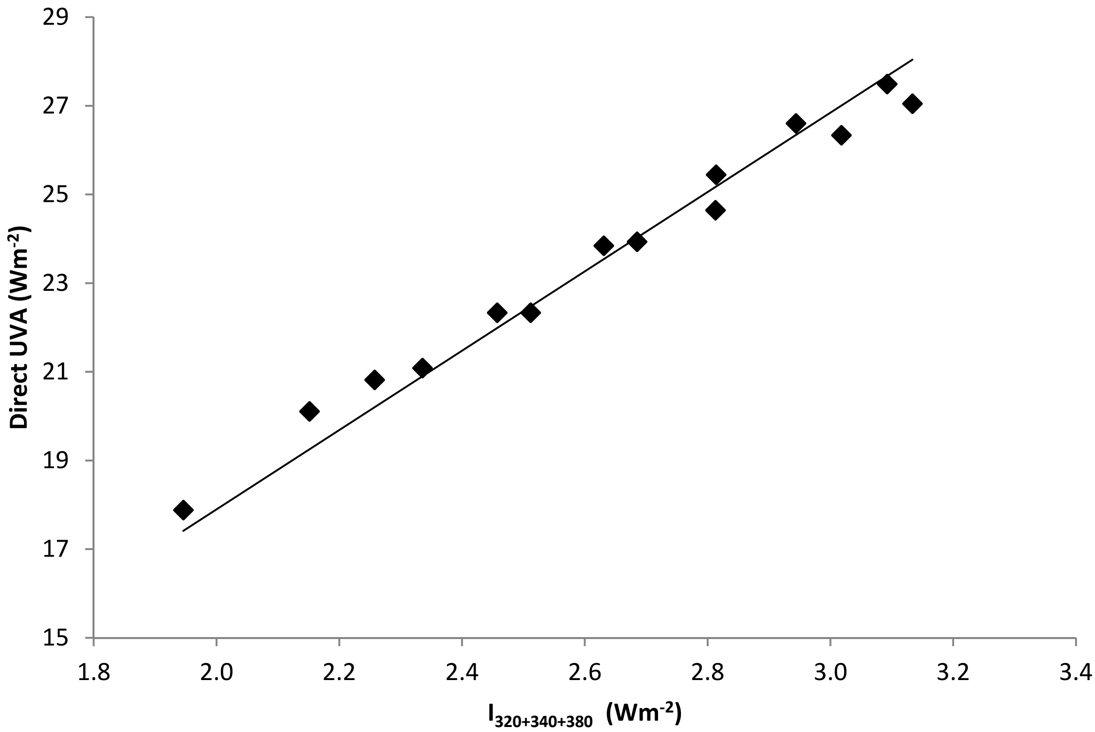

Figure 2: Model for the determination of the broadband direct sun UVA irradiances from the sum of the smartphone derived narrowband direct sun irradiances at 320, 340 and 380 nm.

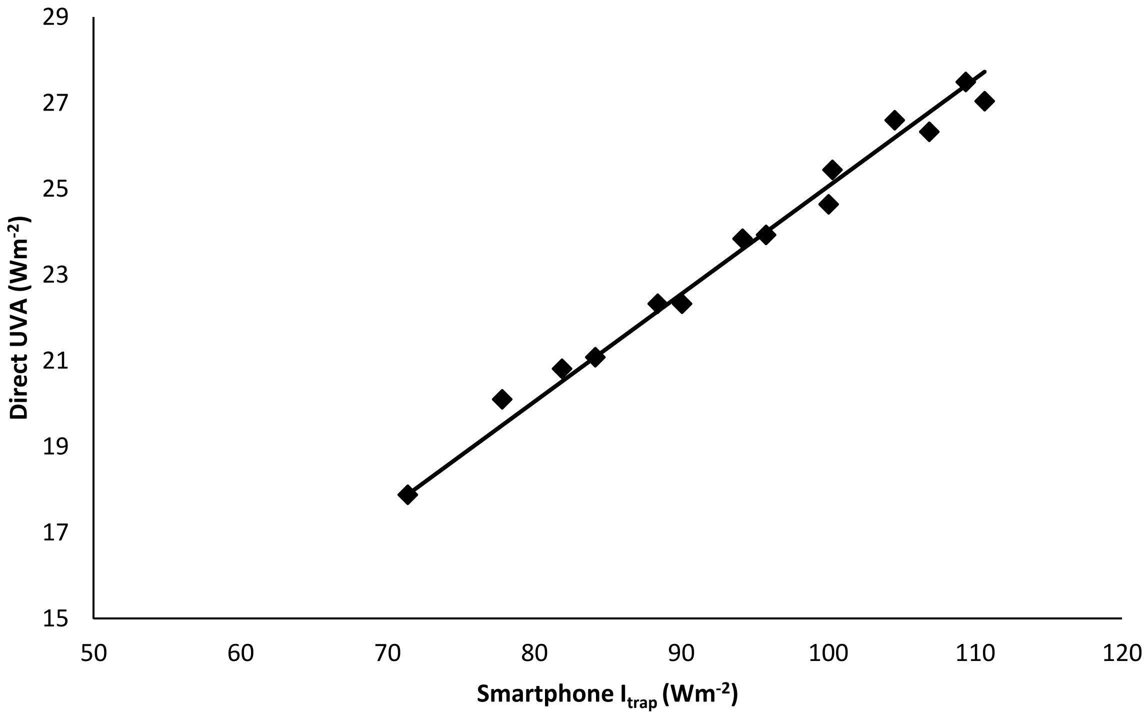

Figure 3: Model for the determination of the broadband direct sun UVA irradiances from the smartphone derived narrowband direct sun irradiances using ($10xI_{320}$ + $30xI_{340}$ + $40xI_{380}$) .

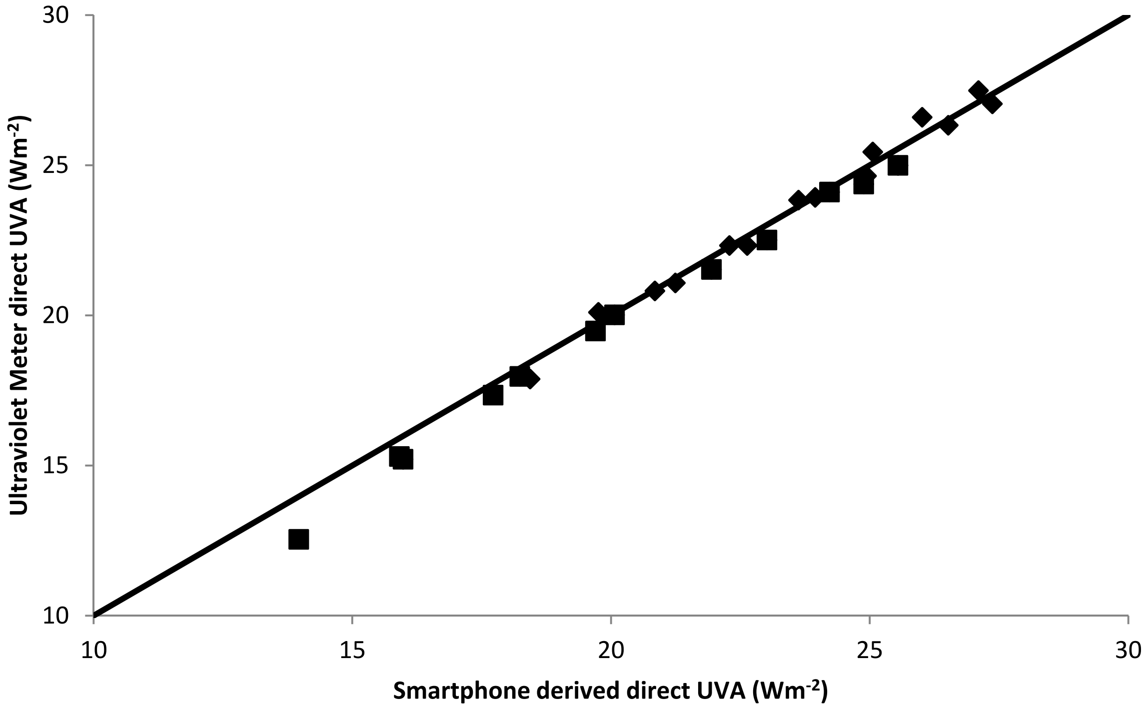

Figure 4: Comparison of smartphone derived direct sun UVA irradiances with corresponding measurements from the ultraviolet meter for validation data with the I_{380} model applied. The boxes and diamonds represent the validation and calibration data respectively and the line represents an exact match.

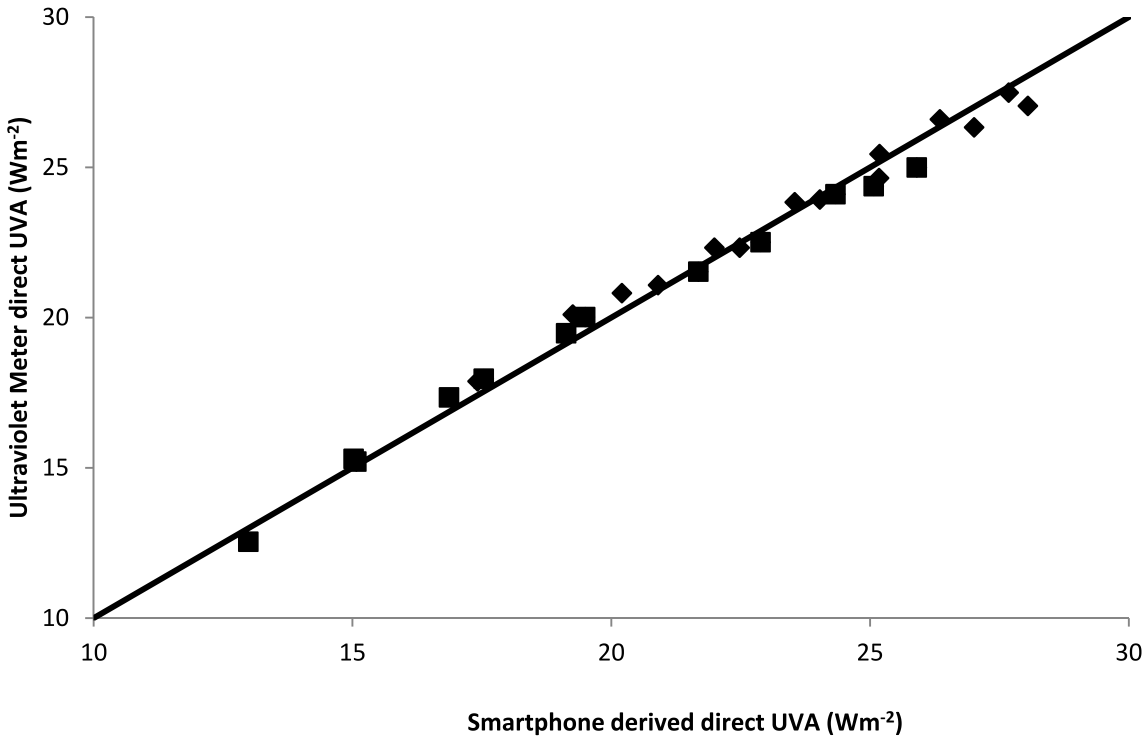

Figure 5: Comparison of smartphone derived direct sun UVA irradiances with corresponding measurements from the ultraviolet meter for validation data with the $(I_{320} + I_{340} + I_{380})$ model applied. The boxes and diamonds represent the validation and calibration data respectively and the line represents an exact match.

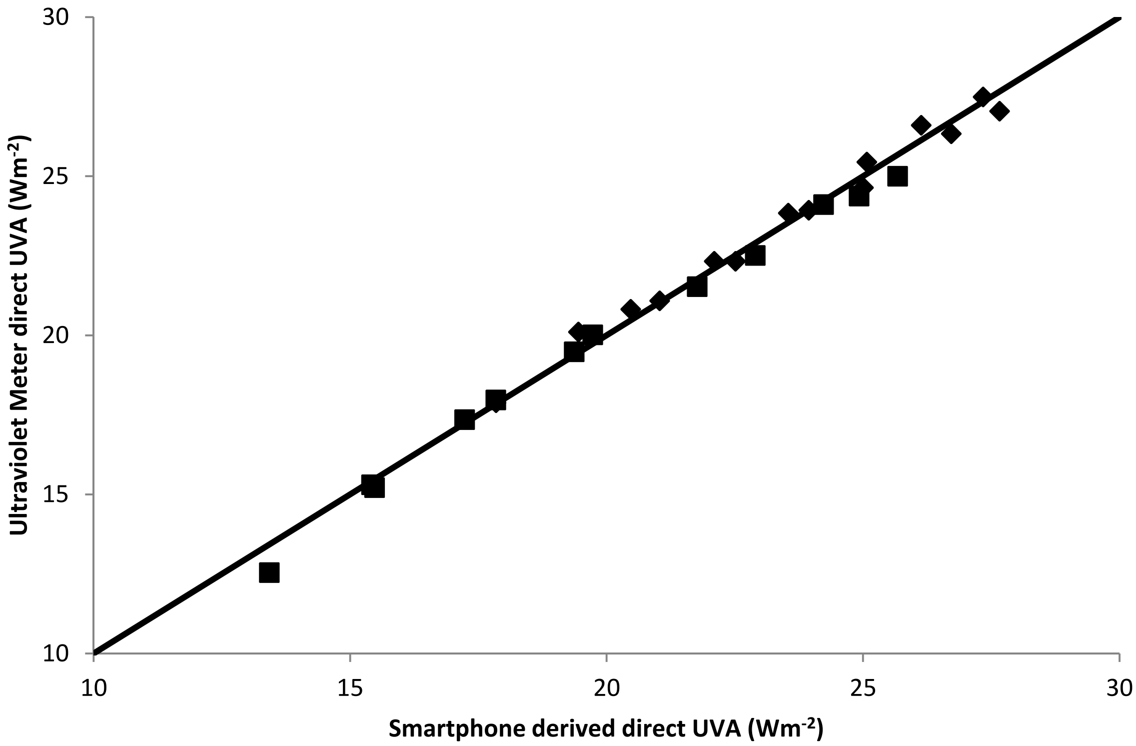

Figure 6: Comparison of smartphone derived direct sun UVA irradiances with corresponding measurements from the ultraviolet meter for validation data with the I_{trap} model applied. The boxes and diamonds represent the validation and calibration data respectively and the line represents an exact match.

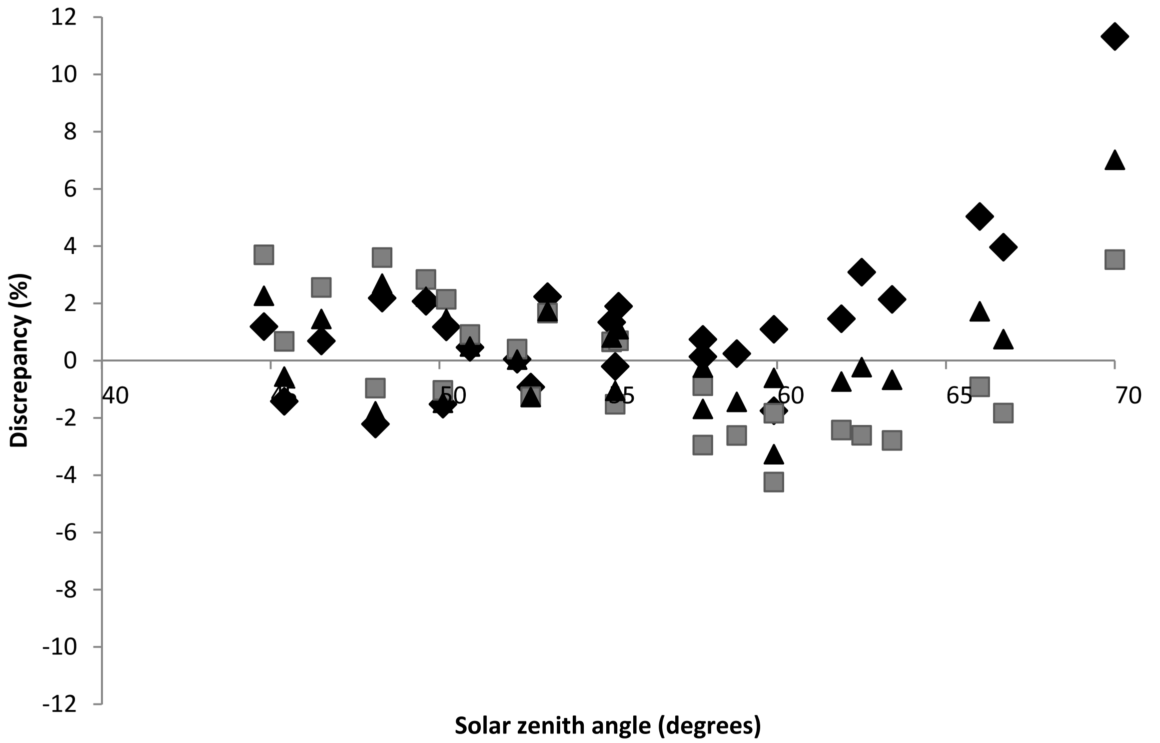

Figure 7: Comparison of percentage discrepancies between the modelled broadband direct sun UVA and observations made by the ultraviolet meter. Diamonds represent the I_{380} model, squares represent the (I_{380} + I_{340} + I_{320}) model and the triangles represent the I_{trap} model.